# Analysis of $(K^-, K^+)$ inclusive spectrum with semiclassical distorted wave model

S. Hashimoto,[1] M. Kohno,[2] K. Ogata,[1] and M. Kawai[1]

[1] *Department of Physics, Kyushu University, Fukuoka 812-8581, Japan*
[2] *Physics Division, Kyushu Dental College, Kitakyushu 803-8580, Japan*

(Dated: November 1, 2006)

The inclusive $K^+$ momentum spectrum in the $^{12}$C$(K^-, K^+)$ reaction is calculated by the semiclassical distorted wave (SCDW) model, including the transition to the $\Xi^-$ bound state. The calculated spectra with the strength of the $\Xi^-$-nucleus potential $-50$, $-20$, and $+10$ MeV are compared with the experimental data measured at KEK with $p_{K^-} = 1.65$ GeV/$c$. The shape of the spectrum is reproduced by the calculation. Though the inclusive spectrum changes systematically depending on the potential strength, it is not possible to obtain a constraint on the potential from the present data. The calculated spectrum is found to have strong emission-angle dependence. We also investigate the incident $K^-$ momentum dependence of the spectrum to see the effect of the Fermi motion of the target nucleons which is explicitly treated in the SCDW method.

PACS numbers: 21.80.+a, 25.80.Nv, 24.10.Eq, 24.50.+g

## I. INTRODUCTION

Hypernuclear physics has been disclosing characteristic features of strong interactions in baryon systems with strangeness. The $\Lambda$-$N$ interaction has been fairly well studied through analyses of experimental data on from light to heavy $\Lambda$ hypernuclei. $\Sigma$-$N$ and $\Xi$-$N$ interactions, however, are not well explored because of insufficient experimental data. In particular, the $\Xi$-$N$ interaction is much ambiguous for this reason despite the fact that its knowledge is the most important for understanding the physics of octet baryons as a probe of the strangeness $S = -2$ sector.

Since the information from direct $Y$-$N$ scattering experiments is extremely limited, the data on the production of a hyperon $Y$ in strangeness exchange reactions $(\pi^+, K^+)$, $(\pi^-, K^+)$, $(K^-, K^+)$ etc. have been a principal source of information on the single-particle potential $U_Y$ felt by $Y$ in the final hypernucleus that reflects the properties of the underlying $Y$-$N$ interaction. The well depth of the $\Xi$-nucleus potential $U_\Xi$ was conjectured to be about 14 MeV by a distorted wave impulse approximation (DWIA) analysis of the inclusive $K^+$ spectra in the threshold region of the $(K^-, K^+)$ reaction [1, 2]. This potential depth is not conclusive, however, because of the limited statistics and resolution. The situation will be improved in the near future, since the $(K^-, K^+)$ experiments with high-intensity $K^-$ beams with a better resolution are prepared in the J-PARC project at KEK.

In the recent papers [3, 4], the inclusive spectra of the $(\pi^-, K^+)$ $\Sigma$ formation reaction were analysed by means of the semiclassical distorted wave (SCDW) model [5] and information on the $\Sigma$-nucleus potential was extracted. In this paper, we calculate, using SCDW, the inclusive $K^+$ spectrum in the $(K^-, K^+)$ $\Xi^-$ production reaction in an attempt to determine the $\Xi^-$-nucleus potential. In view of the on-going experimental progress, we try to elucidate the angle dependence and the incident energy dependence of the inclusive cross section. The SCDW model has been successful in quantitatively describing $(p, p'x)$ and $(p, nx)$ inclusive cross sections for wide range of energy transfers and emission angles without any free adjustable parameter [5, 6, 7]. The single free parameter in the present SCDW calculation of the strangeness exchange reactions is the strength of the $\Xi^-$-nucleus potential $U_Y$.

The formulation of the SCDW model for describing the $(K^-, K^+)$ spectrum is described in Sec. II: for quasifree region in Sec. II A and for bound state region in Sec. II B. In Sec. III, descriptions are given of the kaon distorted waves, the single-particle states of target nucleons and the $\Xi^-$ hyperon, and the strength of the elementary process $K^- + p \to K^+ + \Xi^-$. Numerical results of the calculations for the $(K^-, K^+)$ spectra are compared with the experimental data and discussed in Sec. IV. A summary and conclusions are given in Sec. V.

## II. FORMALISM

### A. SCDW for inclusive spectrum

The inclusive double differential cross section in the center of mass (c.m.) system for the $^{12}$C$(K^-, K^+)$ reaction with production of a $\Xi^-$ hyperon is given in the first order DWIA by

$$\frac{d^2\sigma}{dE_f d\Omega_f} = (2\pi)^4 E_{i,\mathrm{red}} E_{f,\mathrm{red}} \frac{p_f}{p_i} \sum_{\alpha,\beta} \frac{1}{4E_i E_f (2\pi)^6} \times \left| \langle \chi_f^{(-)*}(\boldsymbol{r}) \phi_\beta^*(\boldsymbol{r}) \mid v \mid \chi_i^{(+)}(\boldsymbol{r}) \phi_\alpha(\boldsymbol{r}) \rangle \right|^2 \times \delta(\varepsilon_\beta - \varepsilon_\alpha - \omega)\,, \quad (1)$$

where $E_{c,\mathrm{red}} = E_c E_{c,A}/(E_c + E_{c,A})$ is the reduced energy, $p_c$ is the relative momentum between the kaon and the target $^{12}$C nucleus, $\chi_c^{(+)\mathrm{or}(-)}$ is the distorted wave of the kaon at energy $E_c$ for $c = i$ and $f$ where $i$ and $f$ stand for the initial and the final state, respectively, and $E_{i,A}$ $(E_{f,A})$ is the total energy of the target nucleus (hypernucleus) in the c.m. system. The factor $4E_iE_f(2\pi)^6$ is

the product of the normalization factors of the $\chi_c$ given by

$$\langle\chi_c(\boldsymbol{p}_c)|\chi_c(\boldsymbol{p}'_c)\rangle = 2E_c(2\pi)^3\delta^3(\boldsymbol{p}_c-\boldsymbol{p}'_c)\,. \tag{2}$$

The suffices $\alpha$ and $\beta$ denote the states of the nucleon hole and the unobserved $\Xi^-$ hyperon in the final hypernucleus, respectively, and $\phi_\alpha$ and $\phi_\beta$ are the corresponding single particle wave functions with energies $\varepsilon_\alpha$ and $\varepsilon_\beta$. The delta function guarantees energy conservation where $\omega = E_i - E_f$ is the energy transfer. The $t$-matrix in coordinate representation of the elementary process $K^- + p \to K^+ + \Xi^-$ is denoted by $v$ that depends on energies and momenta of the particles in the reaction. In the present calculation we assume the range of $v$ to be zero.

In the laboratory system, in which most experimental data are given, the cross section is given by

$$\frac{d^2\sigma}{dp_f^{\rm L}d\Omega_f^{\rm L}} = J\frac{d^2\sigma}{dE_f d\Omega_f}\,, \tag{3}$$

where L denotes the laboratory system and $J = \partial(E_f,\Omega_f)/\partial(p_f^{\rm L},\Omega_f^{\rm L})$ is the Jacobian.

Expanding the squared modulus in Eq. (1), one obtains

$$\frac{d^2\sigma}{dp_f^{\rm L}d\Omega_f^{\rm L}} = J(2\pi)^4 E_{i,\rm red}E_{f,\rm red}\frac{p_f}{p_i}\frac{1}{4E_iE_f(2\pi)^6}\int\int d\boldsymbol{r}d\boldsymbol{r}'\,\chi_f^{(-)*}(\boldsymbol{r})v\chi_i^{(+)}(\boldsymbol{r})\chi_f^{(-)}(\boldsymbol{r}')v^*\chi_i^{(+)*}(\boldsymbol{r}')K(\boldsymbol{r},\boldsymbol{r}')\,, \tag{4}$$

where the nonlocal kernel $K(\boldsymbol{r},\boldsymbol{r}')$ is given by

$$\begin{aligned}K(\boldsymbol{r},\boldsymbol{r}') \;=\; &\sum_{\alpha,\,\beta}\phi_\beta^*(\boldsymbol{r})\phi_\alpha(\boldsymbol{r})\phi_\beta(\boldsymbol{r}')\phi_\alpha^*(\boldsymbol{r}')\\ &\times\delta(\varepsilon_\beta-\varepsilon_\alpha-\omega)\,.\end{aligned} \tag{5}$$

The summation over $\alpha$ extends to all the hole states below the Fermi level. The summation over $\beta$ is unrestricted since there is no Pauli principle for the produced hyperon.

For the summation over $\alpha$, we use the Wigner transform

$$\sum_\alpha\phi_\alpha(\boldsymbol{r})\phi_\alpha^*(\boldsymbol{r}') = \sum_{nlj}\int d\boldsymbol{k}_\alpha\,\Phi_{nlj}(\boldsymbol{R},\boldsymbol{k}_\alpha)e^{-i\boldsymbol{k}_\alpha\cdot\boldsymbol{s}}\,, \tag{6}$$

where $\boldsymbol{R} = \frac{\boldsymbol{r}+\boldsymbol{r}'}{2}$ and $\boldsymbol{s} = \boldsymbol{r}'-\boldsymbol{r}$ denote the midpoint and the relative coordinates of $\boldsymbol{r}$ and $\boldsymbol{r}'$, respectively. The summation over $\beta$ is replaced by the integrals

$$\begin{aligned}\sum_\beta\phi_\beta^*(\boldsymbol{r})\phi_\beta(\boldsymbol{r}') \;\to\; &\frac{1}{(2\pi)^3}\int d\Omega_\beta\int d\varepsilon_\beta\frac{1}{2}\left(\frac{2\mu_Y}{\hbar^2}\right)^{3/2}\\ &\times\sqrt{\varepsilon_\beta}\;\;\phi_\beta^*(\boldsymbol{r})\phi_\beta(\boldsymbol{r}')\,,\end{aligned} \tag{7}$$

over the outgoing direction $\Omega_\beta$ and the energy $\varepsilon_\beta$ of the produced hyperon in state $\beta$ in the asymptotic region, and $\mu_Y$ is the reduced mass of the $\Xi^-$-nucleus system in the final state.

In the SCDW model, the local semiclassical approximation (LSCA) is used for the distorted waves $\chi_c$ [5]

$$\chi_c(\boldsymbol{R}\pm\tfrac{1}{2}\boldsymbol{s}) \cong \chi_c(\boldsymbol{R})e^{\pm i\boldsymbol{k}_c(\boldsymbol{R})\cdot\frac{1}{2}\boldsymbol{s}}\,, \tag{8}$$

for small $\boldsymbol{s}/2$, where $\hbar\boldsymbol{k}_c(\boldsymbol{R})$ is the local momentum. The direction of $\boldsymbol{k}_c(\boldsymbol{R})$ is calculated by

$$\hat{\boldsymbol{k}}_c(\boldsymbol{R}) = \frac{{\rm Re}[\chi_{\rm c}^{(\pm)*}(\boldsymbol{R})(-{\rm i})\nabla\chi_{\rm c}^{(\pm)}(\boldsymbol{R})]}{\left|\chi_{\rm c}^{(\pm)}(\boldsymbol{R})\right|^2}\,, \tag{9}$$

and the magnitude is determined by the energy-momentum relation at $\boldsymbol{R}$,

$$\begin{aligned}&\hbar^2c^2k_c^2(\boldsymbol{R}) + 2E_{c,\rm red}(U_R(\boldsymbol{R})+V_{\rm Coul}(\boldsymbol{R}))\\ &\qquad -V_{\rm Coul}^2(\boldsymbol{R}) = E_c^2 - m_K^2c^4\,,\end{aligned} \tag{10}$$

where $m_K$ is the kaon mass 494 MeV/$c^2$, $V_{\rm Coul}(\boldsymbol{R})$ is the Coulomb potential, and $U_R(\boldsymbol{R})$ is the real part of the distorting potential for $\chi_c$ with $E_c$.

The LSCA for the distorted waves $\chi_c$ is expected to work well, because the nonlocal kernel $K(\boldsymbol{r},\boldsymbol{r}')$, which can now be written as

$$\begin{aligned}K(\boldsymbol{R}-\tfrac{1}{2}\boldsymbol{s},\boldsymbol{R}+\tfrac{1}{2}\boldsymbol{s}) \;=\; &\frac{1}{2(2\pi)^3}\left(\frac{2\mu_Y}{\hbar^2}\right)^{3/2}\sum_{nlj}\int d\boldsymbol{k}_\alpha\\ &\times\Phi_{nlj}(\boldsymbol{R},\boldsymbol{k}_\alpha)e^{-i\boldsymbol{k}_\alpha\cdot\boldsymbol{s}}\int d\Omega_\beta\\ &\times\int d\varepsilon_\beta\sqrt{\varepsilon_\beta}\phi_\beta^*(\boldsymbol{R}-\tfrac{1}{2}\boldsymbol{s})\\ &\times\phi_\beta(\boldsymbol{R}+\tfrac{1}{2}\boldsymbol{s})\delta(\varepsilon_\beta-\varepsilon_\alpha-\omega)\,,\end{aligned} \tag{11}$$

is appreciable only for small $\boldsymbol{s}$ because of the completeness $\sum_\beta\phi_\beta^*(\boldsymbol{R}-\boldsymbol{s}/2)\phi_\beta(\boldsymbol{R}+\boldsymbol{s}/2) = \delta(\boldsymbol{s})$. It is noted that the range of the kernel is shorter than in the cases of $(p,p'x)$ and $(p,nx)$, in which the Pauli principle restricts the summation over $\beta$.

In the present calculation, we make use of the LSCA for the unbound wave functions $\phi_\beta$ in the $\Xi^-$-nucleus potential $U_\Xi$, hence, $\phi_\beta(\boldsymbol{R}\pm\boldsymbol{s}/2) \cong \phi_\beta(\boldsymbol{R})\exp[\pm i\boldsymbol{k}_\beta(\boldsymbol{R})\cdot\boldsymbol{s}/2]$

with the direction given from the flux of $\phi_\beta(\boldsymbol{R})$ as in Eq. (9) and the magnitude $k_\beta\big(\boldsymbol{R}\big) = \{2\mu_Y[\varepsilon_\beta - U_\Xi(\boldsymbol{R})]/\hbar^2\}^{1/2}$, where $U_\Xi(\boldsymbol{R})$ is assumed to be real as described in Sec. III. The approximation is valid when $\varepsilon_\beta$ is large compared with $U_\Xi(\boldsymbol{R})$ and $\boldsymbol{k}_\beta\big(\boldsymbol{R}\big)$ is a slowly function of $\boldsymbol{R}$.

Using the approximations described above, the double differential cross section for the inclusive reaction becomes

$$\frac{d^2\sigma}{dp_f^{\rm L}d\Omega_f^{\rm L}} = J\frac{E_{i,\rm red}E_{f,\rm red}}{2(2\pi)^2}\frac{p_f}{p_i}\left(\frac{2\mu_Y}{\hbar^2}\right)^{3/2}\int d\boldsymbol{R}\sum_{nlj}\frac{1}{4E_iE_f}\int d\boldsymbol{k}_\alpha\int d\Omega_\beta\int d\varepsilon_\beta\sqrt{\varepsilon_\beta}\left|\chi_f^{(-)}(\boldsymbol{R})\right|^2\left|\chi_i^{(+)}(\boldsymbol{R})\right|^2|v|^2$$
$$\times\Phi_{nlj}(\boldsymbol{R},\boldsymbol{k}_\alpha)\left|\phi_\beta(\boldsymbol{R})\right|^2\delta\Big(\boldsymbol{k}_f\big(\boldsymbol{R}\big)-\boldsymbol{k}_i\big(\boldsymbol{R}\big)+\boldsymbol{k}_\beta\big(\boldsymbol{R}\big)-\boldsymbol{k}_\alpha\Big)\delta(\varepsilon_\beta-\varepsilon_\alpha-\omega)\,, \tag{12}$$

where the first delta function on the right hand side implies the local momentum conservation.

### B. SCDW for exclusive spectrum

We apply the SCDW model also to the $(K^-,K^+)$ spectrum in the region of bound states of hypernucleus. The differential cross section in the laboratory system for the transition to a $\Xi^-$-$^{11}$B bound state is given by

$$\frac{d\sigma}{d\Omega_f^{\rm L}} = J'(2\pi)^4E_{i,\rm red}E_{f,\rm red}\frac{p_f}{p_i}\int\int d\boldsymbol{r}d\boldsymbol{r}'\,\frac{1}{4E_iE_f(2\pi)^6}\chi_f^{(-)*}(\boldsymbol{r})\phi^*_{\beta'}(\boldsymbol{r})v_{f\beta',\,i\alpha'}\chi_i^{(+)}(\boldsymbol{r})\phi_{\alpha'}(\boldsymbol{r})$$
$$\times\chi_f^{(-)}(\boldsymbol{r}')\phi_{\beta'}(\boldsymbol{r}')v^*_{f\beta',\,i\alpha'}\chi_i^{(+)*}(\boldsymbol{r}')\phi^*_{\alpha'}(\boldsymbol{r}')\,, \tag{13}$$

where $J'=\partial\Omega_f/\partial\Omega_f^{\rm L}$ is the Jacobian. Compared with the inclusive spectrum, this formula has neither the energy delta function nor the summation of $\alpha$ or $\beta$. Corresponding to a transition from proton-hole state $\alpha'$ to a $\Xi^-$-particle state $\beta'$ with the energies $\varepsilon_{\alpha'}$ and $\varepsilon_{\beta'}$, respectively, there should be a spike at the point with the energy transfer $\omega=\varepsilon_{\beta'}-\varepsilon_{\alpha'}$.

We use the Wigner transforms of the product of wave functions of the nucleon hole and those of the hyperon:

$$\phi_{\alpha'}(\boldsymbol{r})\phi^*_{\alpha'}(\boldsymbol{r}') = \int d\boldsymbol{k}_{\alpha'}\,\Phi_{\alpha'}(\boldsymbol{R},\boldsymbol{k}_{\alpha'})e^{-i\boldsymbol{k}_{\alpha'}\cdot\boldsymbol{s}}\,, \tag{14}$$

$$\phi^*_{\beta'}(\boldsymbol{r})\phi_{\beta'}(\boldsymbol{r}') = \int d\boldsymbol{k}_{\beta'}\,\Phi_{\beta'}(\boldsymbol{R},\boldsymbol{k}_{\beta'})e^{i\boldsymbol{k}_{\beta'}\cdot\boldsymbol{s}}\,. \tag{15}$$

Using Eqs. (14) and (15) and changing the variables of integration to ($\boldsymbol{R}$, $\boldsymbol{s}$), one can write Eq. (13) as

$$\frac{d\sigma}{d\Omega_f^{\rm L}} = J'\frac{E_{i,\rm red}E_{f,\rm red}}{(2\pi)^2}\frac{p_f}{p_i}\int d\boldsymbol{R}\,\frac{1}{4E_iE_f}\int d\boldsymbol{k}_{\alpha'}\int d\boldsymbol{k}_{\beta'}\left|\chi_f^{(-)}(\boldsymbol{R})\right|^2\left|\chi_i^{(+)}(\boldsymbol{R})\right|^2|v|^2$$
$$\times(2\pi)^3\Phi_{\alpha'}(\boldsymbol{R},\boldsymbol{k}_{\alpha'})\Phi_{\beta'}(\boldsymbol{R},\boldsymbol{k}_{\beta'})\delta\Big(\boldsymbol{k}_f\big(\boldsymbol{R}\big)-\boldsymbol{k}_i\big(\boldsymbol{R}\big)+\boldsymbol{k}_{\beta'}-\boldsymbol{k}_{\alpha'}\Big)\,. \tag{16}$$

In this case, the nonlocal kernel $K(\boldsymbol{r},\boldsymbol{r}')=\phi_{\alpha'}(\boldsymbol{r})\phi^*_{\alpha'}(\boldsymbol{r}')\phi^*_{\beta'}(\boldsymbol{r})\phi_{\beta'}(\boldsymbol{r}')$ has the range $\boldsymbol{s}$ of the order of the target nuclear radius. Since we still use the LSCA for the $\chi_c$, the accuracy of Eq. (16) depends on that of the LSCA with such large $\boldsymbol{s}$, which will be discussed in Sec. IV B.

## III. WAVE FUNCTIONS AND TRANSITION STRENGTH

The distorted waves of the $K^\pm$ are calculated as solutions of the standard Klein-Gordon equation with distorting potentials $U_c$. The equation in the laboratory system reads

$$\big[\hbar^2c^2\nabla^2_{\boldsymbol{r}}+(p_K^{\rm L})^2c^2-2E_K^{\rm L}(U_c^{\rm L}(\boldsymbol{r})+V_{\rm Coul}^{\rm L}(\boldsymbol{r}))$$
$$+(V_{\rm Coul}^{\rm L}(\boldsymbol{r}))^2\big]\chi_c^{\rm L}(\boldsymbol{r})=0\,, \tag{17}$$

where $\boldsymbol{r}$ is the displacement of the kaon from the center of mass of the target nucleus, $p_K^{\rm L}$ ($E_K^{\rm L}$) is the momentum (energy) of the kaon in the laboratory system, and

$U_c^{\rm L}$ and $V_{\rm Coul}$ are, respectively, the distorting and the Coulomb potentials defined in the laboratory system for the states $c = i$ and $f$. In the present calculation, we approximate Eq. (17) by the equation in the c.m. system

$$\left[\hbar^2 c^2 \nabla^2_{\boldsymbol{r}} + p_c^2 c^2 - 2E_{c,\rm red}(U_c(\boldsymbol{r}) + V_{\rm Coul}(\boldsymbol{r})) + V^2_{\rm Coul}(\boldsymbol{r})\right]\chi_c(\boldsymbol{r}) = 0\,, \qquad (18)$$

replacing $p_K^{\rm L}$, $E_K^{\rm L}$, $U_c^{\rm L}$, and $V_{\rm Coul}$ by $p_c$, $E_{c,\rm red}$, $U_c$, and $V_{\rm Coul}$, respectively, in order to include the nuclear recoil effect. We use distorting potentials of the standard $t\rho$ approximation of Ref. [8]:

$$2E_{c,\rm red}U_c(r) \;=\; -4\pi F_k \left(i\frac{\sigma_{KN}k_{KN}}{4\pi} + {\rm Re}[f_{KN}(0)]\right) \times\rho(r)\,, \qquad (19)$$

where $F_k = M_{c,A}W_{KN}/M(E_c + E_{c,A})$ is a kinematical factor resulting from the transformation of the $KN$ scattering amplitude from the $K$-$N$ to the $K$-nucleus c.m. systems, $\sigma_{KN}$ is the isospin-averaged $KN$ total cross section, $f_{KN}(0)$ is the $KN$ forward scattering amplitude in the free space, and $\rho(r)$ is the nucleon density distribution of the nucleus in the $K$-nucleus c.m. system. The ${\rm Re}[f_{KN}(0)]$ and $\sigma_{KN}$ are obtained as the isospin-average of those given in Ref. [9] in parameterized forms. The masses of the nucleon, the target nucleus, and the hypernucleus are denoted by $M$, $M_{i,A}$, and $M_{f,A}$, respectively, and $W_{KN}$ ($k_{KN}$) denotes the total kaon-nucleon energy (wave number) in their c.m. system.

Actually, the $U_c$ do not agree with the optical potentials $\hat{U}^{\pm}$ that fit the experimental total cross sections $\sigma_{\rm T}$ of $K^{\pm}$. Figure 1 shows the $\sigma_{\rm T}$ for $K^{\pm}$ on $^{12}$C calculated with the $\hat{U}^{\pm}$ (dashed line) and the $U_c$ (solid line). It turns out, however, that the inclusive $(K^-, K^+)$ cross section calculated with the $U_c$ agrees with that calculated with the $\hat{U}^{\pm}$ within 10% which is within the experimental error of the $(K^-, K^+)$ spectrum. We use, therefore, the potentials $U_c$ in our calculations.

The single-particle wave functions and the density distribution function $\rho(r)$ of the target nucleus are calculated in the Hartree-Fock model of Campi and Sprung [11]. The unobserved hyperon $\Xi^-$ is assumed to propagate in a Woods-Saxon potential,

$$U_\Xi(r) = \frac{V_\Xi}{1 + \exp\{(r - R)/a\}} \qquad (20)$$

with $R = 1.1A^{1/3}$ fm and $a = 0.65$ fm. The calculation is performed with a series of $V_\Xi = -50$, $-20$, and $+10$ MeV. The flux of the $\Xi^-$ decreases in the propagation because of its interaction with other nucleons. We take that effect and also the experimental energy resolution into account by means of convolution of the calculated spectra with a Lorentz form of width $\Gamma$.

The transition strength $|v|$ of the elementary process $K^- + p \to K^+ + \Xi^-$ is assumed to be related to the differential cross section in the free space

$$\frac{d\sigma}{d\Omega} = \frac{1}{(4\pi)^2}\frac{E_p E_\Xi}{W^2}\frac{k_{K^+}}{k_{K^-}}\,|v|^2 \qquad (21)$$

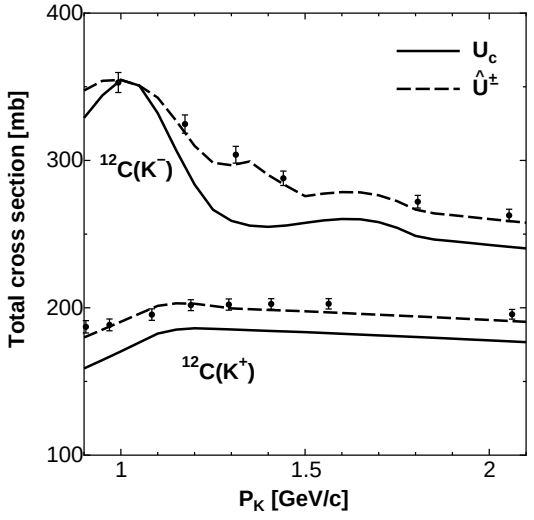


FIG. 1: The total cross sections of the $K^-$ and the $K^+$ collisions on $^{12}$C as functions of the incident momenta of $K^-$ and $K^+$ in the laboratory frame. The optical model values with the $t\rho$ potentials $U_c$ and the optical potentials $\hat{U}^{\pm}$ are represented by the solid lines and the dashed lines, respectively, and compared with the experimental data of Ref. [10].

in the on-shell approximation, where $W$ is the invariant energy, and $E_p$ ($E_\Xi$) is the energy of the proton (the $\Xi^-$ hyperon) and $k_{K^-}$ ($k_{K^+}$) is the momentum of $K^-$ ($K^+$) in the $K^-$-$p$ ($K^+$-$\Xi^-$) c.m. system. We use the elementary cross section parameterized in Ref. [12] as a function of $s$ and the scattering angle $\theta$. In our model described in the previous section, $W$ and $\theta$ are given by the local momenta of the particles $K^-$ and $p$ in the initial state and $K^+$ and $\Xi^-$ in the final state at each collision point $\boldsymbol{R}$.

## IV. RESULTS AND DISCUSSION

### A. Transition to continuum states

In Fig. 2 the momentum spectrum of $K^+$ in $^{12}{\rm C}(K^-, K^+)$ at incident momentum $p_{K^-} = 1.65$ GeV/$c$ calculated with $V_\Xi = -50$ (dotted line), $-20$ (solid line), and $+10$ MeV (dashed line) are compared with the KEK experimental data [13]. Since the data are average over the emission angles $\theta_{K^+}$ between 1.7° and 13.6°, the calculated values are correspondingly averaged. The spectrum shown is after the Lorentzian convolution mentioned in the preceding section. The result turns out to be quite insensitive to the width $\Gamma$ of the convolution. In Fig. 2 the half width $\Gamma/2$ is tentatively taken to be 2 MeV, the same value as for the transitions to bound states discussed later.

The shape of the spectrum is reproduced by the calculation, but the absolute magnitude of the cross section is underestimated by about a factor of 2. A possible

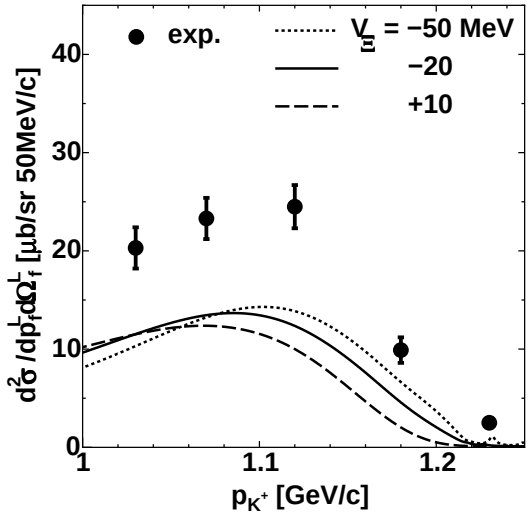


FIG. 2: Momentum spectrum of $K^+$ in $^{12}$C$(K^-, K^+)$ at $p_{K^-} = 1.65$ GeV/$c$ averaged over the emission angles between $\theta_{K^+} = 1.7^\circ$ and $13.6^\circ$. The data of Ref. [13] are compared with theoretical values calculated with $V_\Xi = -50$, $-20$, and $+10$ MeV represented by the curves as indicated.

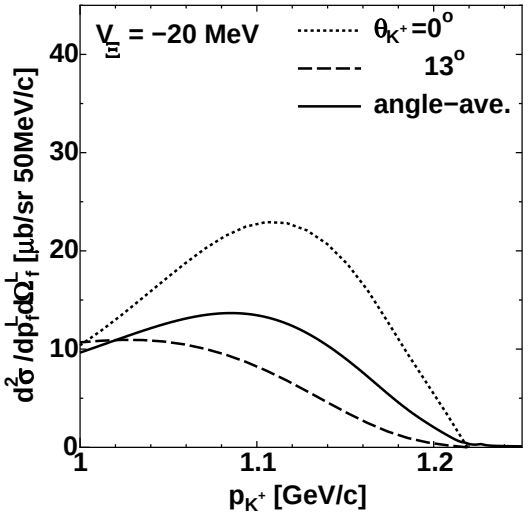


FIG. 3: Emission angle dependence of the momentum spectrum in $^{12}$C$(K^-, K^+)$ at $p_{K^-} = 1.65$ GeV/$c$ with $V_\Xi = -20$ MeV. The spectra at $\theta_{K^+} = 0^\circ$ and $13^\circ$ are shown together with the average over $1.7^\circ < \theta_{K^+} < 13.6^\circ$.

reason on the theoretical side is that we do not correct the lack of the center-of-mass motion of the target wave function. Since the momentum transfer from $K^-$ to $K^+$ is large, the effect is not negligible. This problem in the context of the SCDW method has yet to be clarified. On the physics side, we ignore multi-step processes. Their contributions have been estimated by Nara *et al.* [12] by means of the intranuclear cascade model (INC), and shown to be small in the case of $^{12}$C$(K^-, K^+)$. Since INC is a classical mechanical simulation, however, reinvestigation by means of the quantum mechanical SCDW model is desirable, even though the magnitude of the cross sections in Fig. 2 is almost the same as that of the one-step process in given by the INC calculation of Ref. [12]. Another possible reason for the discrepancy is the in-medium modification of the elementary process which is not taken into account in the calculation. There is also experimental uncertainty of about 30 % in the magnitude of the elementary cross section. Figure 2 shows that the $V_\Xi$-dependence of the angle-averaged spectrum is not very strong. The peak position shifts naturally as the potential strength changes. It is obvious, however, that one hardly determines the value of $V_\Xi$ from the present experimental data.

Figure 3 shows the same calculated momentum spectra as in Fig. 2 at $\theta_{K^+} = 0^\circ$ (dotted line) and $13^\circ$ (dashed line). One sees that the $\theta_{K^+}$ dependence is very strong. This is in contrast to the almost same spectra at $0^\circ$ and $13.6^\circ$ in Ref. [14] obtained with angle-averaged elementary cross sections. This clearly shows the significance of the use of angular dependent elementary cross sections in the present SCDW model calculation.

Figure 4 shows the dependence of the calculated $^{12}$C$(K^-, K^+)$ energy spectrum on the incident momentum $p_{K^-}$, which is not very strong. The dotted, solid, and dashed curves denote the calculated energy spectra at $p_{K^-} = 1.50$, 1.65, and 1.80 GeV/$c$, respectively. It is interesting to note, however, that the change of the position and the hight of the peak with the change of $p_{K^-}$ from 1.50 to 1.80 GeV/$c$ is not simple, unlike that of the elementary cross section of Ref. [12] used in the present calculation. Analysis of the calculation shows that the Fermi motion of the target nucleon is responsible for this somewhat complicated $p_{K^-}$ dependence of the spectrum.

### B. Transition to bound states

If the potential $U_\Xi$ is attractive and sufficiently strong, the hypernuclear system $\Xi^-$-$^{11}$B can have bound states. Table I shows the energy eigenvalues of the single-particle states of $\Xi^-$ in $U_\Xi$ for the depth of $V_\Xi = -20$ and $-50$ MeV. Transitions to states with a nucleon hole in the $0s_{1/2}^{-1}$-orbit are treated with the convolution of the calculated spectra with the wide width of 9.2 MeV [15]. DWIA calculations of the $(K^-, K^+)$ cross sections are made as in the case of transitions to continuous states (TCS), except that the LSCA is not used to the $\Xi^-$ bound state wave functions. Figure 5 shows the calculated momentum spectra of $K^+$ at $p_{K^-} = 1.65$ GeV/$c$ and $\theta_{K^+} = 8^\circ$ in the region of $p_{K^+}$ where the peaks corresponding to the bound states appear. The calculated spectrum is convoluted by Lorentzian with the half width $\Gamma/2 = 2$ MeV which is the sum of 1 MeV due to the decay $\Xi^- p \to \Lambda\Lambda$ and 1 MeV due to the resolution of the detector in the experiment.

In Fig. 5, the dotted, solid, and dashed lines corre-

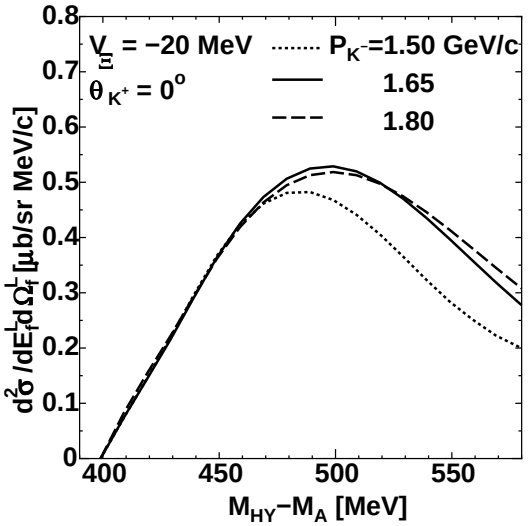


FIG. 4: The energy spectrum of $K^+$ at $\theta_{K^+} = 0^\circ$ at $p_{K^-} =$ 1.50, 1.65, and 1.80 GeV/$c$ calculated with $V_\Xi = -20$ MeV and $\Gamma/2 = 0$, are plotted as functions of $M_{HY} - M_A$ where $M_{HY}$ and $M_A$ are the masses of the hypernucleus and the target nucleus, respectively.

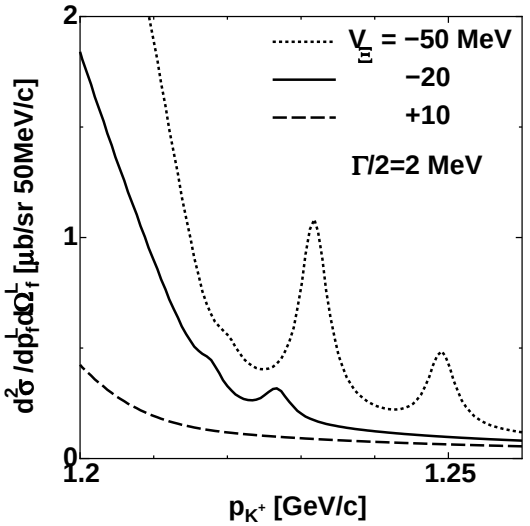


FIG. 5: The $^{12}$C$(K^-, K^+)$ spectra near the $\Xi^-$-$^{11}$B hypernuclear bound state region at $p_{K^-} = 1.65$GeV/$c$ and $\theta_{K^+} = 8^\circ$ calculated with $V_\Xi = -50$, $-20$, and $+10$ MeV.

TABLE I: Eigenstates and eigenenergies of $\Xi^-$ in the single-particle potential $U_\Xi$.

| $V_\Xi$ [MeV] | $E_\Xi$ [MeV] | | |
|---|---|---|---|
| | $0s$-state | $0p$-state | $1s$-state |
| $-20$ | $-8.3$ | $-0.6$ | — |
| $-50$ | $-28.7$ | $-13.0$ | $-2.6$ |

spond to the calculated spectra with $V_\Xi = -50$, $-20$, and $+10$ MeV, respectively. One sees two (three) peaks corresponding to the transitions from the $0p_{3/2}^{-1}$-state to the $0s$- and $0p$-states ($0s$-, $0p$- and $1s$-states) in Table I for $V_\Xi = -20$ ($-50$) MeV, while for $V_\Xi = +10$ MeV, as anticipated, there is no peak.

An essential difference from the case of TCS is that there is no summation over the final states and, consequently, no short ranged kernel discussed in Sec. II that would restrict the distance of the source points of the outgoing distorted waves $\chi_f$ that can interfere with each other. Therefore, one needs the LSCA extrapolation of $\chi_f$ over a long distance, the validity of which needs to be examined. Numerical tests show that the accuracy of the LSCA extrapolation from a point on the nuclear surface to another point across the nuclear diameter is within about a factor of 2. This is the sort of accuracy of the calculations shown in Fig. 5.

The presence of a bound state peak in the spectrum shows that the $\Xi^-$-nucleus interaction is attractive and strong enough to support that particular bound state. Through the model calculation, one can estimate the strength of the peak that can suggest the experimental precision required for measuring it. In this regard, we consider what the results of the present work suggest is significant despite the numerical ambiguities discussed above.

## V. SUMMARY AND CONCLUSIONS

The inclusive $K^+$ momentum spectrum in the $^{12}$C$(K^-, K^+)$ reaction is calculated by the semiclassical distorted wave (SCDW) model. The same method of the calculation is used as in our previous works on $(\pi^-, K^+)$ and $(\pi^+, K^+)$ inclusive spectra [3, 4]. The transition to the $\Xi^-$ bound state is also considered. The accuracy of the local semiclassical approximation (LSCA) for the discrete part of the spectrum is not so good as for the continuous part, but the error is estimated to be within a factor of 2. The standard $t\rho$ potentials are used for the $K^\pm$-$^{12}$C distorting potentials. Although the total cross sections of the $K^-$ and $K^+$ scatterings on $^{12}$C calculated with those potentials do not reproduce the experimental data very well, the resulting $(K^-, K^+)$ spectra agree with the ones calculated with the optical potentials $\hat{U}^\pm$ within about 10 %. In order to improve a model for kaon distorted waves, one needs more experimental data in the momentum region of interest.

Since we can explicitly take into account the dependences of the elementary $K^- + p \to K^+ + \Xi^-$ cross section on the invariant mass squared and the scattering angle, the present calculation is more realistic than those, e.g. in Ref. [14], in which some constant average value of the elementary cross section is employed. The $\Xi^-$-nucleus potential is assumed to be of a Woods-Saxon form. The inclusive momentum spectra with the strength of the $^{12}$C$(K^-, K^+)$ reaction calculated with the strength of the potential $V_\Xi = -50$, $-20$, and $+10$ MeV are compared with the experimental data at $p_{K^-} = 1.65$

GeV/$c$. The shape of the spectrum is reproduced by the calculation. However, the magnitude of the cross section is underestimated by about a factor of 2. Though the inclusive spectrum changes systematically depending on the strength of $V_\Xi$, it is not possible to obtain a constraint on $V_\Xi$ from the present analysis on the basis of the available data.

There are several possible reasons for the underestimation. There should be the contribution of the multi-step processes to $(K^-, K^+)$. We will investigate, in the next step, the influence of the multi-step processes by means of the SCDW model for these processes [16]. The effect of in-medium modifications of the elementary process may not be negligible, although it can reduce the cross section. Another source of the discrepancy is experimental uncertainty of about 30 % in the elementary cross sections used in the calculations. It is obvious that we need experimental data of the $(K^-, K^+)$ spectrum and the elementary cross sections with better accuracy for a more quantitatively reliable analysis.

The calculated spectrum is found to have strong emission-angle dependence. When analyzing $(K^-, K^+)$ experimental spectra with angle-averaging involved, it is important to be aware of such dependence. It is seen from the spectra calculated at incident momenta of $p_{K^-} = 1.50$, 1.65, and 1.80 GeV/$c$ that the cross section at the lower side of the excitation energy hardly depends on the $K^-$ incident momentum. The close examination of the calculation shows that this consequence is due to the Fermi motion of the target nucleons, which is properly treated in our SCDW framework. The discrete part of the spectrum of $K^+$ will be useful for extracting information on the $\Xi^-$-nucleus potential from the future $(K^-, K^+)$ experimental data, because the possibility to detect a peak structure below the threshold has not been ruled out yet experimentally.

### Acknowledgments

The authors would like to thank T. Fukuda and A. Ohnishi for valuable discussions. This study is supported by Grants-in-Aid for Scientific Research from the Japan Society for the Promotion of Science (Grant Nos. 18042004 and 17540263).

[1] T. Fukuda *et al.*, Phys. Rev. C **58**, 1306 (1998).
[2] P. Khaustov *et al.*, Phys. Rev. C **61**, 054603 (2000).
[3] M. Kohno, Y. Fujiwara, Y. Watanabe, K. Ogata, and M. Kawai, Prog. Theor. Phys. **112**, 895 (2004).
[4] M. Kohno, Y. Fujiwara, Y. Watanabe, K. Ogata, and M. Kawai, to be published in Phys. Rev. C.
[5] Y. L. Luo and M. Kawai, Phys. Lett. **B235**, 211 (1990); Phys. Rev. C **43**, 2367 (1991).
[6] Y. Watanabe *et al.*, Phys. Rev. C **59**, 2136 (1999); Phys. Rev. C **63**, 019901(E) (2000).
[7] K. Ogata, M. Kawai, Y. Watanabe, Sun Weili, and M. Kohno, Phys. Rev. C **60**, 054605 (1999); Phys. Rev. C **63**, 019902(E) (2000).
[8] E. Friedman, A. Gal, and J. Mareš, Nucl. Phys. **A625**, 272 (1997).
[9] A. Sibirtsev and W. Cassing, Nucl. Phys. **A641**, 476 (1998).
[10] D. V. Bugg *et al.*, Phys. Rev. **168**, 1466 (1968).
[11] X. Campi and D. W. Sprung, Nucl. Phys. **A194**, 401 (1972).
[12] Y. Nara, A. Ohnishi, T. Harada, and A. Engel, Nucl. Phys. **A614**, 433 (1997).
[13] T. Iijima *et al.*, Nucl. Phys. **A546**, 588 (1992).
[14] S. Tadokoro, H. Kobayashi, and Y. Akaishi, Phys. Rev. C **51**, 2656 (1995).
[15] H. Tyŕen, S. Kullander, O. Sundberg, R. Ramachandran, and P. Isacsson, Nucl. Phys. **79**, 321 (1966).
[16] M. Kawai and H. A. Weidenmüller, Phys. Rev. C **45**, 1856 (1992).